

# Kinetic and thermodynamic studies of adsorption of $\text{Cu}^{2+}$ and $\text{Pb}^{2+}$ onto amidoximated bacterial cellulose

Shiyan Chen · Wei Shen · Feng Yu · Huaping Wang

Received: 12 November 2008 / Revised: 14 April 2009 / Accepted: 19 April 2009 /  
Published online: 29 April 2009  
© Springer-Verlag 2009

**Abstract** Removal of  $\text{Cu}^{2+}$  and  $\text{Pb}^{2+}$  from aqueous solutions by adsorption onto amidoximated bacterial cellulose (Am-BC) was investigated. The effects of pH, initial concentration, contact time and temperature were studied in batch experiments. The pseudo-first and pseudo-second orders and intraparticle diffusion equation were used to evaluate the kinetic data and the constants were determined. The experimental data fits well to the pseudo-second order kinetic model, which indicates that the chemical adsorption is the rate-determining step, instead of mass transfer. The equilibrium adsorption data were described by the Langmuir, Freundlich, and Temkin isotherms. The Am-BC showed a better fit to the Langmuir isotherm. The separation factor ( $R_L$ ) revealed the favorable nature of the isotherm. The thermodynamic parameters ( $\Delta H_{\text{ads}}^0$ ,  $\Delta S_{\text{ads}}^0$ ,  $\Delta G_{\text{ads}}^0$ ) for  $\text{Cu}^{2+}$  and  $\text{Pb}^{2+}$  adsorption onto Am-BC were also determined from the temperature dependence. The values of enthalpy and entropy indicated that this process was spontaneous and exothermic. The experimental studies indicate that Am-BC would be a potential effective adsorbent to remove the metal ions from wastewater.

**Keywords** Adsorption · Kinetics · Thermodynamics · Amidoximated bacterial cellulose

## Introduction

With the rapid increase in global industrial activities, heavy metal pollution has become serious [1]. Heavy metals may come from various industrial sources such as

---

S. Chen · W. Shen · F. Yu · H. Wang (✉)  
State Key Laboratory for Modification of Chemical Fibers and Polymer Materials,  
College of Materials Science and Engineering, Donghua University,  
201620 Shanghai, People's Republic of China  
e-mail: wanghp@dhu.edu.cn

electroplating, metal finishing, textile, storage batteries, lead smelting, mining, plating, ceramic and glass industries.  $\text{Cu}^{2+}$  and  $\text{Pb}^{2+}$  are common contaminants of industrial wastewaters. Because they pose serious environmental problems and are dangerous to human health, considerable attention has been paid to methods for their removal from industrial wastewaters [2, 3].

There are various methods for removing heavy metals including chemical precipitation, membrane filtration, ion exchange, liquid extraction or electrodialysis [4, 5]. However, these methods are not widely used due to their high cost and low feasibility for small-scale industries [6]. In contrast, the adsorption technique is one of the preferred methods for removal of heavy metals because of its efficiency and low cost [7]. Conventional adsorbents such as granular or powdered activated carbon are not always popular as they are not economically viable and technically efficient [8]. Non-conventional materials have been tested in a large scale for this purpose, such as concrete materials [9], lignite [10], tree fern [11], etc.

In this research, amidoximated bacterial cellulose (Am-BC) was used as an adsorbent to remove  $\text{Cu}^{2+}$  and  $\text{Pb}^{2+}$  from aqueous solutions. Bacterial cellulose (BC) is an extracellular cellulose produced by bacteria of genus *Acetobacter* [12]. It is composed of microfibrils, which have a ribbon-like structure, and the thickness ( $0.1 \times 10^{-6}$  m) is two orders of magnitude smaller than that of plant cellulose ( $10 \times 10^{-6}$  m). In addition, the microfibrils retain a fine network structure. BC has been studied to introduce amine, or phosphonic groups on the surfaces for adsorbing some metal ions from aqueous solutions [13], but the adsorption capacity is far from approving. In this work, we focused on BC as a starting material to prepare a new adsorbent, Am-BC, and investigate the adsorption properties. A series of experiments have been performed to characterize heavy metals adsorption equilibrium on Am-BC. Three different kinds of kinetic models (intraparticle diffusion models, pseudo-first-order and second-order equations) were selected to determine which of these mechanisms predominates in heavy metals adsorption by Am-BC. Equilibrium adsorption isotherms were analyzed to obtain the Langmuir, Freundlich, and Temkin constants. Full thermodynamic investigations were also undertaken. This information will be useful for further application for the metal ions' removal.

## Experimental

### Materials

Am-BC was prepared in our laboratory according to the method reported by Saliba and Gauthier [14]. Acrylonitrile, hydroxylamine, sodium carbonate, and the salts of copper and lead ( $\text{CuSO}_4 \cdot 5\text{H}_2\text{O}$ ,  $\text{Pb}(\text{NO}_3)_2$ ) used in the experiments were purchased from Sinopharm Chemical Reagent Co. Ltd. Deionized water was used for the preparation of the standard solutions for the adsorption tests. The standards for analysis were prepared from stock solutions of 1,000 ppm supplied by Shanghai Institute of Measurement and Testing Technology.

## Fourier transform infrared (FTIR) spectroscopy

The powder of BC, cyanoethyl bacterial cellulose (CE-BC) and Am-BC were dried at 50 °C under vacuum firstly. And the samples were prepared mixing 1 mg of material with 100 mg of spectroscopy grade KBr, dried at 50 °C under vacuum, and pressed into a small tablet. FT-IR spectra were recorded on a NEXUS-670 Nicolet FTIR instrument equipped with a MCT detector in the absorption mode with a resolution of 4 cm<sup>-1</sup>, in the range of 4,000–400 cm<sup>-1</sup>.

## Elemental analysis

The amount of amidoxime groups grafted on BC was calculated based on the nitrogen content, determined by an elemental analyzer (Germany Elemental Analysensysteme GmbH, Vario EL III).

## Adsorption experiments

Batch adsorption experiments were conducted in 50 ml flasks. Am-BC (0.02 g) was added into 10 ml solution with a desired pH value (adjusted with 0.1 M NaOH or 0.1 M HNO<sub>3</sub>) and a known metal ion concentration (made by CuSO<sub>4</sub>·5H<sub>2</sub>O or Pb(NO<sub>3</sub>)<sub>2</sub>). The mixture was shaken in a thermostatic water-bath shaker operated at 298.15 K and 200 rpm. Samples were taken at predetermined time intervals for the analysis of metal ion concentrations in the solution until adsorption equilibrium was reached. The concentrations of Cu<sup>2+</sup> and Pb<sup>2+</sup> ions in the samples were analyzed with an atomic absorption spectrophotometer (ZEE nit 700, German). The initial concentrations of metal ion in all of the test solutions were 200 mg/l, but the initial pH values of the solutions were different, ranging from 2 to about 7. The amount of metal ions adsorbed on the adsorbent at adsorption equilibrium and the distribution constant  $K_D$  (ml/g) were calculated from the following equations [15]:

$$q_e = (C_0 - C_e)V/W \quad (1)$$

$$K_D = m_{\text{ads}}V/m_{\text{sol}}W \quad (2)$$

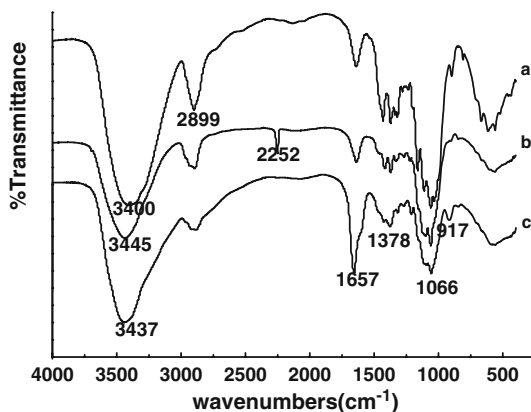
where  $C_0$  and  $C_e$  are the initial and equilibrium metal ions concentrations (mg/l), respectively,  $m_{\text{ads}}$  and  $m_{\text{sol}}$  are the amount of metal in adsorbent and in solution (mg),  $V$  is the volume of the solution (l) and  $W$  is the weight of the Am-BC used (g).

## Results and discussion

### FTIR spectroscopy

FT-IR spectra are a useful tool to identify the presence of certain functional groups in a molecule as each specific chemical bond often has a unique energy absorption band. The FT-IR spectra of BC, CE-BC, Am-BC are shown in Fig. 1. The peaks at 1,066 and 2,899 cm<sup>-1</sup> corresponding to C–O–C and C–H stretching bands are

**Fig. 1** FT-IR spectra of BC (a), CE-BC (b), Am-BC (c)



observed in all the samples. The major peak located at around  $3,400\text{ cm}^{-1}$  in BC (Fig. 1a) is attributed to  $-\text{OH}$  stretching vibration. When cyano groups were grafted onto BC, a sharp peak appeared at  $2,252\text{ cm}^{-1}$  is observed in CE-BC shown in Fig. 1b. Then the peak disappeared and two new absorption peaks at  $1,657$  and  $917\text{ cm}^{-1}$  appeared in Am-BC (Fig. 1c), corresponding to the stretching vibration of  $\text{C}=\text{N}$  and  $\text{N}-\text{OH}$  bonds, respectively. The phenomena indicated that cyano groups were converted to amidoxime groups by reaction with hydroxylamine. Moreover, the peak at around  $3,445\text{ cm}^{-1}$  becomes broader compared with that of BC which might come from the combination of the stretching vibration bands of both  $-\text{OH}$  and  $-\text{NH}_2$  groups. Besides, the increase of intensity around  $1,378\text{ cm}^{-1}$  related to the  $\text{N}-\text{H}$  bending band is observed, which also confirms the existence of  $-\text{NH}_2$  in Am-BC.

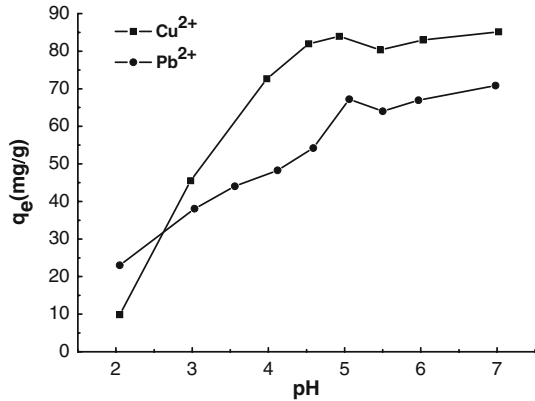
### Elemental analysis

Nitrogen content is 7.99% in CE-BC by elemental analysis, and 12.63% in Am-BC. Under similar reaction condition, a nitrogen content of amidoximated plant cellulose is only 6.12%, which is similar to what Saliba and Gauthier [14] have reported. The results suggested that the amination (%) can be influenced by the morphology of cellulose. As BC microfibrils are much thinner than fibers of plant cellulose, much more reactive hydroxyl groups on the surface of BC can be functionalized.

### Effect of pH on adsorption

Figure 2 shows the experimental results for the  $\text{Cu}^{2+}$  and  $\text{Pb}^{2+}$  removal under various initial solution pH values at adsorption equilibriums. The pH values were varied between  $2 \pm 0.1$  and  $7 \pm 0.1$ . It shows that the adsorption capacity increases significantly with the increase of pH when pH values less than 5.0. When pH value is between 5.0 and 5.5,  $\text{Cu}^{2+}$  and  $\text{Pb}^{2+}$  adsorption onto Am-BC decreases with the increase of solution pH values. The maximum adsorption capacity of  $\text{Cu}^{2+}$  and  $\text{Pb}^{2+}$  are found to be 84 and 67 mg/g, respectively, which is obviously higher than

**Fig. 2** The effect of pH on the amount of  $\text{Cu}^{2+}$  and  $\text{Pb}^{2+}$  adsorbed onto Am-BC. Initial metal ion concentration 200 mg/l, pH  $2 \pm 0.1 - 7 \pm 0.1$ , amount of Am-BC 0.02 g

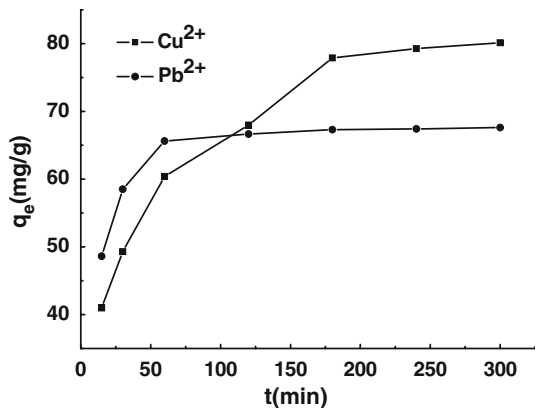


the amidoximated cellulose previously reported [14]. The value is also higher or can be compared with other adsorbents such as chitosan, dead microbial biomass, and agriculture waste materials easily available as adsorbents [16, 17]. From pH 5.5–7.0, the amount of adsorption increases again with the increase of solution pH values, which might be resulted from the precipitation of  $\text{Cu}^{2+}$  and  $\text{Pb}^{2+}$  at higher pH values. From the results, we can conclude that pH values play an important role in the  $\text{Cu}^{2+}$  and  $\text{Pb}^{2+}$  adsorption onto Am-BC.

#### Effect of adsorption time

The adsorption mixture set in constant temperature ( $T = 298.15$  K) was sampled at different time ranging from 15 to 300 min to investigate the effect of contact time on the adsorption rate. The result was plotted in Fig. 3. A rapid adsorption was observed at the initial stage and more than 70% of the  $\text{Cu}^{2+}$  and 90% of the  $\text{Pb}^{2+}$  were adsorbed during the first 60 min. The adsorption equilibrium was established after 180 min.

**Fig. 3** The effect of contact time on the amount of  $\text{Cu}^{2+}$  and  $\text{Pb}^{2+}$  adsorbed onto Am-BC. Initial metal ion concentration 200 mg/l, pH  $5 \pm 0.1$ , amount of Am-BC 0.02 g



## Adsorption kinetics

In order to investigate the mechanism of adsorption, the pseudo-first order, pseudo-second order and intraparticle diffusion model were used to study the obtained experimental data. The pseudo-first order model of Lagergren is given as [18]:

$$-\ln\left(1 - q_t/q_e\right) = k_1 t \quad (3)$$

where  $q_e$  and  $q_t$  are the amounts of metal ions adsorbed onto Am-BC (mg/g) at equilibrium and at time  $t$ , respectively, and  $k_1$  is the rate constant of first-order adsorption (1/min). The straight-line plots of  $-\ln(1 - q_t/q_e)$  against  $t$  were used to determine the rate constant,  $k_1$  and correlation coefficients,  $R^2$ . In many cases, the first-order equation of Lagergren does not fit well to the whole range of contact time. It would only be applicable at the initial stage of the adsorption process [19]. Figure 4 represents the pseudo-first order plots for Am-BC.

The pseudo-second order model can be expressed as [18]:

$$t/q_t = 1/k_2 q_e^2 + t/q_e \quad (4)$$

where  $k_2$  is the rate constant of second-order adsorption (g/mg min). The straight-line plots of  $t/q_t$  against  $t$  were used to determine the rate constant ( $k_2$ ) and correlation coefficient ( $R^2$ ). Figure 5 represents the pseudo-second order plots for Am-BC. This model is more likely to predict the adsorption behavior over the whole time range of adsorption and is in agreement with chemical adsorption being the rate-controlling step [20], which may involve valency forces through sharing or exchange of electrons between metal ions and adsorbent.

Based on the data from Table 1, it was found that the correlation coefficients for the pseudo-first order kinetic model were lower than those of the pseudo-second order kinetic model, which means the pseudo-second order kinetic model fits better on the real adsorption process. The pseudo-second order assumes that chemisorptions were the rate controlling mechanism. Both of the pseudo-first and pseudo-second order cannot identify the diffusion mechanism; thereby the kinetic results were further analyzed using intraparticle diffusion equation.

**Fig. 4** Pseudo-first order plot for the adsorption of  $\text{Cu}^{2+}$  and  $\text{Pb}^{2+}$  onto Am-BC

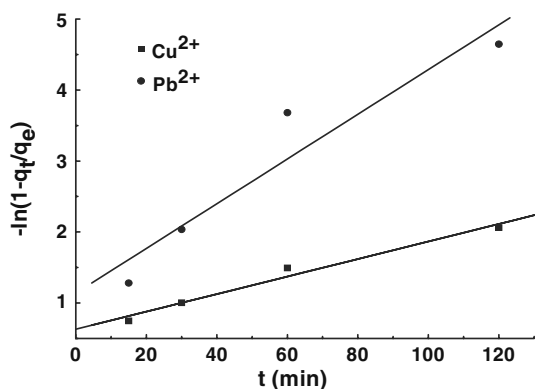


**Fig. 5** Pseudo-second order plot for the adsorption of  $\text{Cu}^{2+}$  and  $\text{Pb}^{2+}$  onto Am-BC

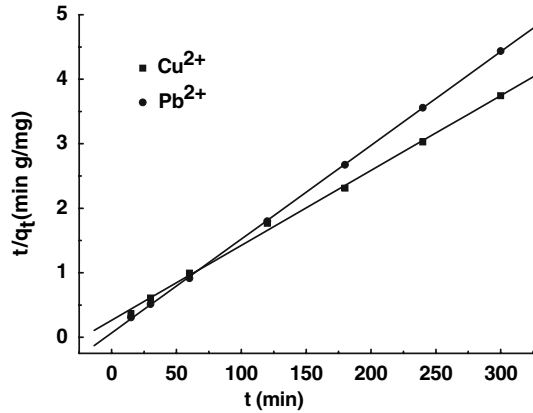


**Table 1** Pseudo-first, pseudo-second-order and intraparticle diffusion equation constants and values of  $R^2$  for the adsorption of  $\text{Cu}^{2+}$  and  $\text{Pb}^{2+}$  onto Am-BC

| Metal ion        | Pseudo-first order model |               |         | Pseudo-second order model |              |         | Intraparticle diffusion equation       |        |  |        |
|------------------|--------------------------|---------------|---------|---------------------------|--------------|---------|--|--------|--|--------|
|                  | $C_0$ (mg/l)             | $k_1$ (1/min) | $R_1^2$ | $k_2$ (g/mg min)          | $q_e$ (mg/g) | $R_2^2$ | $k_{int,1}$ (mg/g min <sup>1/2</sup> ) | $R^2$  | $k_{int,2}$ (mg/g min <sup>1/2</sup> ) | $R^2$  |
| $\text{Cu}^{2+}$ | 200                      | 0.0124        | 0.9889  | 0.0005                    | 86.13        | 0.9989  | 5.0014                                 | 0.9998 | 1.8459                                 | 0.8970 |
| $\text{Pb}^{2+}$ | 200                      | 0.0315        | 0.9556  | 0.0031                    | 68.82        | 0.9999  | 4.3067                                 | 0.9813 | 0.1406                                 | 0.9452 |

The adsorbate can be transferred from the solution phase to the surface of the adsorbent in several steps. The steps may include film or external diffusion, pore diffusion, surface diffusion and adsorption on the pore surface. The overall adsorption can occur through one or more steps. The intraparticle diffusion equation is given by the equation [21]:

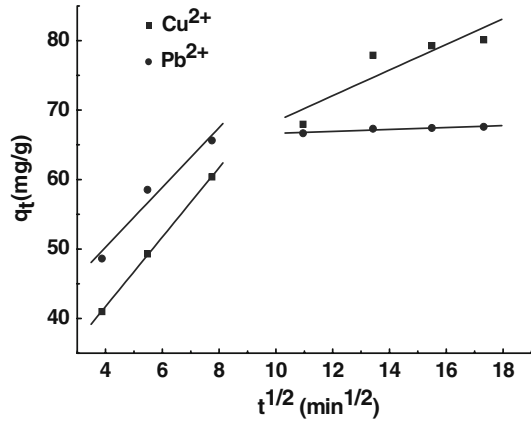
$$q_t = k_{int}t^{1/2} \tag{5}$$

where  $q_t$  is the amount of metal ions adsorbed onto Am-BC (mg/g) at time  $t$ , and  $k_{int}$  is the intraparticle diffusion rate constant (mg/g min<sup>1/2</sup>). The straight-line plots of  $q_t$  against  $t^{1/2}$  were used to determine the intraparticle diffusion rate,  $k_{int}$  and correlation coefficient,  $R^2$ .

Figure 6 represents the plot for the intraparticle diffusion equation for Am-BC. The straight-line plot for all the obtained data showed a first straight line portion which represents macropore diffusion and the second one represents micropore diffusion.

According to the Eq. 5, if the plot gives a straight line, the adsorption is controlled solely by the intraparticle diffusion. Nevertheless, if the adsorption data shows multilinear plots (shown in Fig. 6), it indicates that there are two or more steps involving in the adsorption process [22]. If the lines pass through the origin, it indicates that intraparticle diffusion is the rate-controlling step. In the present study, the slope of the first straight line was used to derive the values for  $k_{int,1}$  and the

**Fig. 6** Intraparticle diffusion kinetics for the adsorption of  $\text{Cu}^{2+}$  and  $\text{Pb}^{2+}$  onto Am-BC

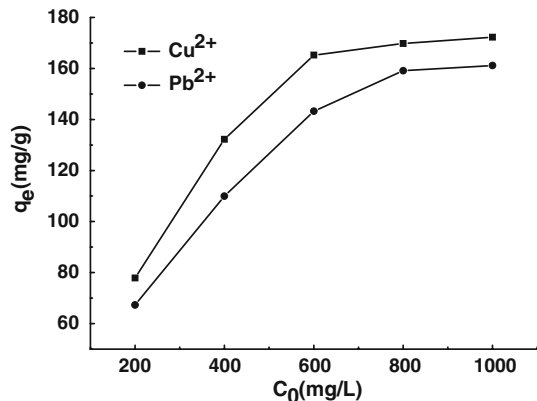


slope for the second one was used to obtain the  $k_{\text{int}, 2}$  value. Based on Table 1,  $k_{\text{int}, 1} > k_{\text{int}, 2}$  can be seen which indicated that the lines did not pass the origin and it shows that intraparticle diffusion is not the rate-controlling step [23, 24]. Moreover, it can be concluded that Am-BC shows a very good correlation coefficient to the first portion of the straight line, which represents macropore diffusion. And the plot showed a curvature which is normally attributed to boundary layer diffusion effect or external mass transfer effects [22].

### Adsorption isotherms

Adsorption isotherms describe how adsorbates interact with adsorbents and are important in optimizing the use of adsorbents. The experimental adsorption data of  $\text{Cu}^{2+}$  and  $\text{Pb}^{2+}$  on the Am-BC are shown in Fig. 7. The results clearly indicate that with an increase of initial  $\text{Cu}^{2+}$  and  $\text{Pb}^{2+}$  concentration, the adsorption capacity of both  $\text{Cu}^{2+}$  and  $\text{Pb}^{2+}$  increases significantly. At lower initial metal ions concentration, the adsorption capacities increase linearly with the initial metal ions

**Fig. 7** Adsorption capacities of metal ions onto the Am-BC at various initial metal ions concentrations (initial solution pH 5)





concentration, suggesting that the adsorption sites on the Am-BC are sufficient, and in this case, the amount of adsorption is dependent on the number of metal ions transported from the bulk solution to the surfaces of the Am-BC. At higher initial metal ions concentration, however, the adsorption capacities no longer increase proportionally with the initial metal ions concentration, indicating that the number of adsorption sites on the surfaces of the Am-BC actually limit the adsorption capacities.

The adsorption data have been subjected to different adsorption isotherms, namely the Freundlich, Temkin and Langmuir models. These models suggest different adsorption modes with different interactions between the adsorbed molecules or ions. In the case of the Freundlich models, the energetic distribution of sites is heterogeneous, due to the diversity of adsorption sites or the diverse nature of the metal ions adsorbed, free or hydrolyzed species. The Temkin isotherm model assumes that the heat of adsorption of all the molecules or ions in the layer decreases linearly with the thickness of the coverage due to the sorbate/adsorbate interactions. The Langmuir model supposes a monolayer adsorption with a homogenous distribution of adsorption sites and adsorption energies, without interactions between the adsorbed molecules or ions. In order to optimize the design of a adsorption system to remove metal ions from effluents, it is important to establish the most appropriate correlation for the equilibrium curve. Three isotherm equations have been tested in the present study, namely, Freundlich, Temkin and Langmuir.

### The Freundlich isotherm

The well-known Freundlich isotherm [25] is often used for heterogeneous surface energy systems. The form of the Freundlich equation is given as:

$$q_e = K_F C_e^{1/n} \quad (6)$$

This expression can be linearized to give

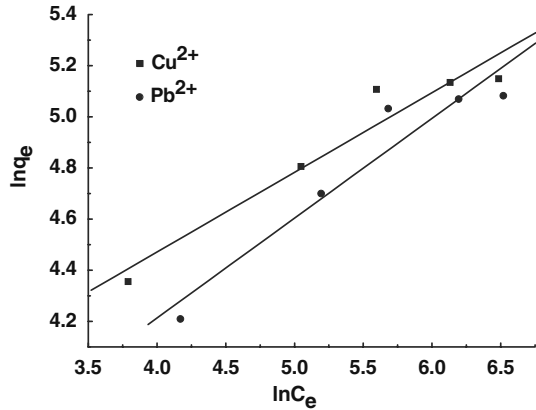
$$\ln q_e = \ln K_F + \left(\frac{1}{n}\right) \ln C_e \quad (7)$$

where  $K_F$  and  $n$  are Freundlich constants indicating adsorption capacity and intensity, respectively. Freundlich model considers a multi-layer adsorption pattern. It also assumes that the adsorbent has energetically heterogeneous surface and has different affinity for adsorption [26]. The values of the Freundlich constants together with the correlation coefficient were presented in Table 2 and the theoretical

**Table 2** Isotherm constants and values of  $R^2$  for the adsorption of  $\text{Cu}^{2+}$  and  $\text{Pb}^{2+}$  onto Am-BC

| Metal ion        | Langmuir parameter |              |        | Freundlich parameter |      |        | Temkin parameter |           |        |
|------------------|--------------------|--------------|--------|----------------------|------|--------|------------------|-----------|--------|
|                  | $b$ (l/mg)         | $q_m$ (mg/g) | $R^2$  | $K_F$                | $n$  | $R^2$  | $B$              | $A$ (l/g) | $R^2$  |
| $\text{Cu}^{2+}$ | 0.0150             | 191.94       | 0.9976 | 25.16                | 3.21 | 0.9659 | 36.77            | 0.2214    | 0.9701 |
| $\text{Pb}^{2+}$ | 0.0090             | 191.57       | 0.9950 | 14.18                | 2.56 | 0.9594 | 42.42            | 0.0797    | 0.9853 |

**Fig. 8** Freundlich adsorption isotherm of adsorption  $\text{Cu}^{2+}$  and  $\text{Pb}^{2+}$  onto Am-BC. Temperature 298.15 K; pH  $5.0 \pm 0.1$ ; amount of Am-BC 0.02 g



Freundlich isotherm was plotted in Fig. 8. The plot is in linear agreement with the correlation coefficient ( $R^2$ ) of 0.9659 and 0.9594 for  $\text{Cu}^{2+}$  and  $\text{Pb}^{2+}$ , respectively. It can be concluded that the Freundlich isotherm is not fit for the adsorption isotherm perfectly under the testing conditions.

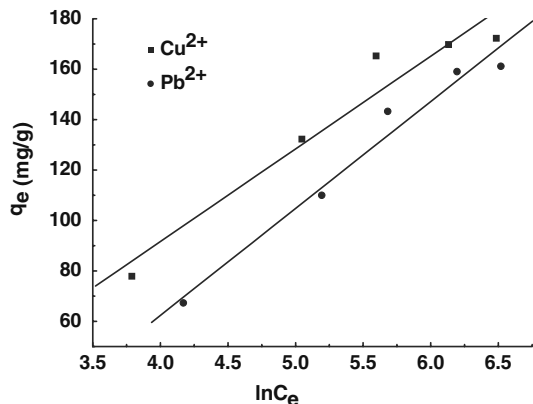
The Temkin isotherm

The Temkin isotherm [27, 28] has been used in many sorption processes. A linear form of the Temkin isotherm can be expressed as:

$$q_e = RT/b \ln A + RT/b \ln C_e \quad (8)$$

where  $RT/b = B$ . The adsorption data can be analyzed according to Eq. 8. Therefore a plot of  $q_e$  versus  $\ln C_e$  enables one to determine the constants A and B. The values of the Temkin constants A and B were listed in Table 2 and the theoretical plot of this isotherm was shown in Fig. 9. The correlation coefficient was also listed in Table 2. From the slope the value of B was evaluated as 36.77 and 42.42 for  $\text{Cu}^{2+}$  and  $\text{Pb}^{2+}$ , respectively. And the value of A was calculated as

**Fig. 9** Temkin adsorption isotherm of adsorption  $\text{Cu}^{2+}$  and  $\text{Pb}^{2+}$  onto Am-BC. Temperature 298.15 K; pH  $5.0 \pm 0.1$ ; amount of Am-BC 0.02 g



0.2214 and 0.0797 (l/g) for  $\text{Cu}^{2+}$  and  $\text{Pb}^{2+}$  from the intercept. It is clear from the plot that the Temkin isotherm can not be used to describe the adsorption isotherm suitably.

### The Langmuir isotherm

The widely used Langmuir isotherm [29] has found successful application in many real adsorption processes and its linear form is expressed as:

$$C_e/q_e = C_e/q_m + 1/bq_m \quad (9)$$

where  $C_e$  is the equilibrium concentration of remaining metal ions in the solution (mg/l);  $q_e$  is the amount of metal ions adsorbed per mass unit of adsorbent at equilibrium (mg/g);  $q_m$  is the amount of metal ions at complete monolayer (mg/g) and  $b$ , the Langmuir constant related to the affinity of binding sites (l/mg) and is a measure of the energy of adsorption. The model assumes that the binding sites are homogeneously distributed over the adsorbent surface. These binding sites have the same affinity for adsorption of a single molecular layer. The binding to the adsorption sites can be either chemical or physical but must be strong enough to prevent displacement of the adsorbed molecules [30].

The values of the Langmuir constants  $q_m$ , and  $b$  with the correlation coefficients were listed in Table 2. The theoretical Langmuir isotherm was plotted in Fig. 10. The monolayer saturation capacities for  $\text{Cu}^{2+}$  and  $\text{Pb}^{2+}$ ,  $q_m$ , were 191.94 and 191.57 mg/g, respectively. Based on the  $b$  values (Langmuir constant related to the affinity of binding sites), Am-BC showed a higher affinity for  $\text{Cu}^{2+}$  ions. This correlated well with the higher adsorption capacity obtained for the Am-BC. The value of the correlation coefficient was higher than the other two isotherms values. In this case, the Langmuir equation represents the best fit of experimental data than the other isotherm equations.

Additionally, an important parameter,  $R_L$ , called the equilibrium parameter was calculated to identify whether an adsorption system is favorable or unfavorable [31, 32].

**Fig. 10** Langmuir adsorption isotherm of adsorption  $\text{Cu}^{2+}$  and  $\text{Pb}^{2+}$  onto Am-BC. Temperature 298.15 K; pH  $5.0 \pm 0.1$ ; amount of Am-BC 0.02 g

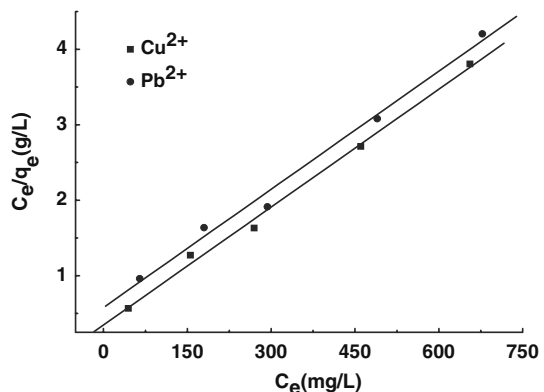
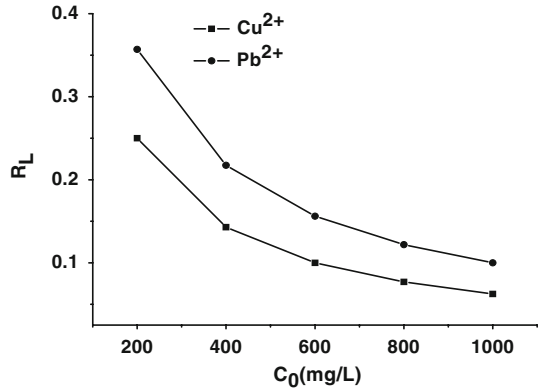


**Fig. 11** Separation factor  $R_L$  for the adsorption of  $\text{Cu}^{2+}$  and  $\text{Pb}^{2+}$  onto Am-BC



$$R_L = 1/(1 + bC_0) \quad (10)$$

where  $b$  is the Langmuir constant and  $C_0$  is the initial concentration (mg/l), the  $R_L$  values between 0 and 1 indicates favorable adsorption. The values of  $R_L$  for adsorption of  $\text{Cu}^{2+}$  and  $\text{Pb}^{2+}$  onto Am-BC are shown in Fig. 11. They indicate that adsorption of metal ions is more favorable at higher initial concentrations than at lower ones.

#### Effect of the temperature on adsorption

The effect of temperature on the adsorption of  $\text{Cu}^{2+}$  and  $\text{Pb}^{2+}$  was studied from 298.15 to 333.15 K. The results are presented in Fig. 12. It can be observed that the amounts of  $\text{Cu}^{2+}$  and  $\text{Pb}^{2+}$  adsorption decreased with the increase of the temperature, which indicates that the process is exothermic in nature. Further, the adsorption is favored at lower temperature.

**Fig. 12** Effect of temperature on  $\text{Cu}^{2+}$  and  $\text{Pb}^{2+}$  adsorption onto Am-BC. Initial metal ions concentration 200 mg/l; pH  $5.0 \pm 0.1$ ; temperature 298.15–333.15 K; amount of Am-BC 0.02 g

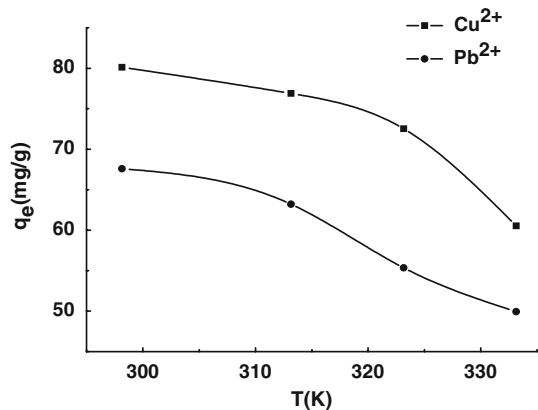
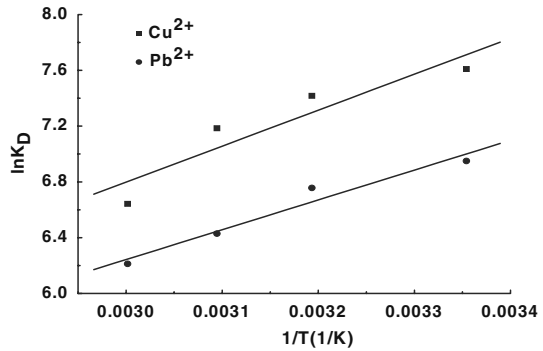


**Fig. 13** Graphical determination of  $\Delta H_{\text{ads}}^0$  and  $\Delta S_{\text{ads}}^0$



**Thermodynamics studies**

The thermodynamic parameters for the adsorption process were calculated using the equation [33, 34]:

$$\ln K_D = \Delta S_{\text{ads}}^0/R - \Delta H_{\text{ads}}^0/RT \tag{11}$$

where  $K_D$  is the distribution coefficient (ml/g),  $\Delta S_{\text{ads}}^0$  is standard entropy (J/mol K),  $\Delta H_{\text{ads}}^0$  is standard enthalpy (kJ/mol),  $T$  is the absolute temperature (K), and  $R$  is the gas constant (8.314 J/mol K).

The experiments were carried out at 298.15, 313.15, 323.15, and 333.15 K with a metal ions concentration of 200 mg/l. The values of  $\Delta H_{\text{ads}}^0$  and  $\Delta S_{\text{ads}}^0$  were calculated from the slopes and intercepts of linear regression of  $\ln K_D$  versus  $1/T$  (Fig. 13). The standard Gibbs free energy  $\Delta G_{\text{ads}}^0$  values (kJ/mol) were calculated from the equation:

$$\Delta G_{\text{ads}}^0 = \Delta H_{\text{ads}}^0 - T\Delta S_{\text{ads}}^0 \tag{12}$$

The values of  $\Delta H_{\text{ads}}^0$ ,  $\Delta S_{\text{ads}}^0$ , and  $\Delta G_{\text{ads}}^0$  are listed in Table 3. In fact, the negative value of enthalpy change  $\Delta H_{\text{ads}}^0$  for the processes further confirms the exothermic nature of the process, the negative entropy of adsorption  $\Delta S_{\text{ads}}^0$  confirms the decreased randomness at the solid–solution interface during adsorption which reflects the affinity of the adsorbent material toward metal ions, and the negative free energy values  $\Delta G_{\text{ads}}^0$  indicate the feasibility of the process and its spontaneous nature without an induction period.

**Table 3** Thermodynamic parameters for the adsorption of Cu<sup>2+</sup> and Pb<sup>2+</sup> onto Am-BC

| Metal ion        | C <sub>0</sub><br>(mg/l) | $\Delta H_{\text{ads}}^0$<br>(kJ/mol) | $\Delta S_{\text{ads}}^0$<br>(J/mol K) | $\Delta G_{\text{ads}}^0$ (kJ/mol) |          |          |          |
|------------------|--------------------------|---------------------------------------|--|------------------------------------|----------|----------|----------|
|                  |                          |                                       |  | 298.15 K                           | 313.15 K | 323.15 K | 333.15 K |
| Cu <sup>2+</sup> | 200                      | -21.46                                | -7.86                                  | -19.12                             | -19.00   | -18.92   | -18.84   |
| Pb <sup>2+</sup> | 200                      | -17.79                                | -1.46                                  | -17.35                             | -17.33   | -17.32   | -17.30   |

## Conclusions

In conclusion, Am-BC was synthesized and characterized by FT-IR and element analysis. The capacity of Am-BC in adsorption  $\text{Cu}^{2+}$  and  $\text{Pb}^{2+}$  was investigated. The experimental data showed that Am-BC was a good metal ions adsorbent which had shown the best adsorption performance for  $\text{Cu}^{2+}$  and  $\text{Pb}^{2+}$  in the solution of pH  $5.0 \pm 0.1$ . The adsorption process was fast. It reached the adsorption equilibrium within 180 min. The adsorption kinetics closely followed the pseudo-second order kinetic model, which assumes that chemisorptions are the rate controlling mechanism. Meanwhile, based on the intraparticle diffusion equation, it can be concluded that the adsorption process follows macropore diffusion and boundary layer diffusion or external mass transfer effects. The adsorption isotherms could be well fitted by the Langmuir equation. Based on Langmuir isotherms, the maximum monolayer adsorption capacity for  $\text{Cu}^{2+}$  and  $\text{Pb}^{2+}$  were 191.94 and 191.57 mg/g, respectively. The dimensionless separation factor  $R_L$  had shown that Am-BC could be used for removal of  $\text{Cu}^{2+}$  and  $\text{Pb}^{2+}$  from aqueous solutions. The temperature was found to have an inverse effect on adsorption of  $\text{Cu}^{2+}$  and  $\text{Pb}^{2+}$ . Thermodynamic constants were also evaluated using equilibrium constants changing with temperature. The negative value of  $\Delta G_{\text{ads}}^0$ ,  $\Delta H_{\text{ads}}^0$  and  $\Delta S_{\text{ads}}^0$  indicated the spontaneity, the exothermic nature, and the probability of favorable nature of adsorption, respectively. The results of the present investigation show that Am-BC is a potentially useful adsorbent for the adsorption of the metal ions.

**Acknowledgments** This work was financially supported by Programme of Introducing Talents of Discipline to Universities (111-2-04, B07024), New Century Excellent Talents in University (NCET-05-0420) and Shanghai Leading Academic Discipline Project (B603).

## References

1. Chen JP, Wang L (2004) Characterization of metal adsorption kinetic properties in batch and fixed-bed reactors. *Chemosphere* 54:397–404
2. Keskinan O, Goksu MZL, Yuceer A, Basibuyuk M, Forster CF (2003) Heavy metal adsorption characteristics of a submerged aquatic plant (*Myriophyllum spicatum*). *Process Biochem* 39:179–183
3. Wan Ngh WS, Endud CS, Mayanar R (2002) Removal of copper(II) ions from aqueous solution onto chitosan and cross-linked chitosan beads. *React Funct Polym* 50:181–190
4. Reardon EJ, Wang Y (2000) A limestone reactor for fluoride removal from wastewaters. *Environ Sci Technol* 34:3247–3253
5. Amor Z, Bariou B, Mameri N, Taky M, Nicolas S, Elmidaoui A (2001) Fluoride removal from brackish water by electrodialysis. *Desalination* 133:215–223
6. Vasconcelos HL, Fávere VT, Gonçalves NS, Laranjeira MCM (2007) Chitosan modified with Reactive Blue 2 dye on adsorption equilibrium of Cu(II) and Ni(II) ions. *React Funct Polym* 67:1052–1060
7. Garcia L, Torrent A, Anticó E, Fontás C, Roglans A (2008) Selective Pd(II) and Pt(IV) sorption using novel polymers containing azamacrocyclic functional groups. *React Funct Polym* 68:1088–1096
8. Gupta SS, Bhattacharyya KG (2006) Removal of Cd(II) from aqueous solution by kaolinite, montmorillonite and their poly(oxo zirconium) and tetrabutylammonium derivatives. *J Hazard Mater* 128:247–257
9. Oguz E (2005) Adsorption of fluoride on gas concrete materials. *J Hazard Mater* 117:227–233
10. Arslan G, Pehlivan E (2008) Uptake of  $\text{Cr}^{3+}$  from aqueous solution by lignite-based humic acids. *Bioresour Technol* 99:7597–7605

11. Ho YS (2003) Removal of copper ions from aqueous solution by tree fern. *Water Res* 37:2323–2330
12. Hestrin S, Schramm M (1954) Synthesis of cellulose by *Acetobacter xylinum*. *Biochem J* 58:345–353
13. Oshima T, Kondo K, Ohto K, Inoue K, Baba Y (2008) Preparation of phosphorylated bacterial cellulose as an adsorbent for metal ions. *React Funct Polym* 68:376–383
14. Saliba R, Gauthier H, Gauthier R, Petit-Ramel M (2000) Adsorption of copper(II) and chromium(III) ions onto amidoximated cellulose. *J Appl Polym Sci* 75:1624–1635
15. Çavuş S, Gürdağ G, Yaşar M, Güçlü K, Gürkaynak MA (2006) The competitive heavy metal removal by hydroxyethyl cellulose-g-poly(acrylic acid) copolymer and its sodium salt: the effect of copper content on the adsorption capacity. *Polym Bull* 57:445–456
16. Wan Ngah WS, Hanafiah MAKM (2008) Removal of heavy metal ions from wastewater by chemically modified plant wastes as adsorbents: a review. *Bioresour Technol* 99:3935–3948
17. Babel S, Kurniawan TA (2003) Low-cost adsorbents for heavy metals uptake from contaminated water: a review. *J Hazard Mater B* 97:219–243
18. Ho YS, McKay G (1998) Kinetic models for the sorption of dye from aqueous solution by wood. *Process Saf Environ Protect* 76:183–191
19. Ho YS, McKay G (1999) The sorption of lead(II) ions on peat. *Water Res* 33:578–584
20. Ho YS, McKay G (1999) Pseudo-second order model for sorption processes. *Process Biochem* 34:451–465
21. Allen SJ, McKay G, Khader KYH (1989) Intraparticle diffusion of a basic dye during adsorption onto sphagnum peat. *Environ Pollut* 56:39–50
22. Srivastava VC, Swamy MM, Mall ID, Prasad B, Mishra IM (2006) Adsorptive removal of phenol by bagasse fly ash and activated carbon: equilibrium, kinetics and thermodynamics. *Colloids Surf A Physicochem Eng Aspects* 272:89–104
23. Özcan A, Özcan AS, Tunali S, Akar T, Kiran I (2005) Determination of the equilibrium, kinetic and thermodynamic parameters of adsorption of copper(II) ions onto seeds of *Capsicum annum*. *J Hazard Mater* 124:200–208
24. Öcan A, Öncü EM, Özcan AS (2006) Kinetics, isotherm and thermodynamic studies of adsorption of Acid Blue 193 from aqueous solutions onto natural sepiolite. *Colloids Surf A Physicochem Eng Aspects* 277:90–97
25. Freundlich HMF (1906) Über die Adsorption in Lösungen. *Z Phys Chem* 57:385–470
26. Papageorgiou SK, Katsaros FK, Kouvelos EP, Nolan JW, Le Deit H, Kanellopoulos NK (2006) Heavy metal sorption by calcium alginate beads from *Laminaria digitata*. *J Hazard Mater* 137:1765–1772
27. Özacar M (2003) Equilibrium and kinetic modelling of adsorption of phosphorus on calcined alunite. *Adsorption* 9:125–132
28. Allen SJ, Gan Q, Matthews R, Johnson PA (2003) Comparison of optimized isotherm models for basic dye adsorption by kudzu. *Bioresour Technol* 88:143–152
29. Langmuir I (1918) The adsorption of gases on plane surfaces of glass, mica and platinum. *J Am Chem Soc* 40:1361–1403
30. Al-Asheh S, Banat F, Al-Omari R, Duvnjak Z (2000) Predictions of binary sorption isotherms for the sorption of heavy metals by pine bark using single isotherm data. *Chemosphere* 41:659–665
31. Bhatnagar A, Jain AK (2005) A comparative adsorption study with different industrial wastes as adsorbents for the removal of cationic dyes from water. *J Colloid Interface Sci* 281:49–55
32. Al-Rub FAA, Kandah M, Al-Dabaybeh N (2002) Nickel removal from aqueous solutions using sheep manure wastes. *Eng Life Sci* 2:111–116
33. Donat R, Akdogan A, Erdem E, Cetisli H (2005) Thermodynamics of  $Pb^{2+}$  and  $Ni^{2+}$  adsorption onto natural bentonite from aqueous solutions. *J Colloid Interface Sci* 286:43–52
34. Gök O, Özcan A, Erdem B, Özcan AS (2008) Prediction of the kinetics, equilibrium and thermodynamic parameters of adsorption of copper(II) ions onto 8-hydroxy quinoline immobilized bentonite. *Colloids Surf A Physicochem Eng Aspects* 317:174–185